Functional connectivity between medial pulvinar and cortical networks as a predictor of arousal to noxious stimuli during sleep

Hélène Bastuji, Andéol Cadic-Melchior, Lucien Ruelle-Le Glaunec, Michel Magnin, Luis Garcia-Larrea

Functional connectivity between medial pulvinar and cortical networks as a predictor of arousal to noxious stimuli during sleep

***Abbreviated* title:** Associative thalamus and pain-induced arousal

Hélène Bastuji[1,2], Andéol Cadic-Melchior [1], Lucien Ruelle-Le Glaunec [1], Michel Magnin[1] and Luis Garcia-Larrea[1,3]

[1] Central Integration of Pain (NeuroPain) Lab - Lyon Neuroscience Research Center, INSERM U1028; CNRS, UMR5292; Université Claude Bernard; Bron, F-69677, France; [2] Centre du Sommeil, Hospices Civils de Lyon, Bron, F-69677, France; [3] Centre d'évaluation et de traitement de la douleur, Hôpital Neurologique, Lyon, France

***Corresponding author**: Hélène Bastuji: Email: bastuji@univ-lyon1.fr

Keywords: nociceptive stimulus, sleep, arousal, thalamus, intracerebral EEG, human

Author Contributions
H.B., A.C.M., L.R.L. and L.G.L. designed research; H.B., A.C.M., L.R.L. and L.G.L. performed research; H.B., A.C.M., L.R.L. and L.G.L. analysed data; H.B., M.M., and L.G.L. wrote the paper.

This manuscript includes:

26 pages, 3 figures and 4 tables. Abstract: 226 words.

Conflict of interest

The authors declare no competing financial interests.

Summary:

The interruption of sleep by a nociceptive stimulus is favoured by an increase in the pre-stimulus functional connectivity between sensory and higher-level cortical areas. In addition, stimuli inducing arousal also trigger a widespread EEG response reflecting the coordinated

activation of a large cortical network. Since functional connectivity between distant cortical areas is thought to be underpinned by trans-thalamic connections involving associative thalamic nuclei, we investigated the possible involvement of one principal associative thalamic nucleus, the medial pulvinar (PuM), in the sleeper's responsiveness to nociceptive stimuli. Intra-cortical and intra-thalamic signals were analysed in 440 iEEG segments during nocturnal sleep in 8 epileptic patients receiving laser nociceptive stimuli. The spectral coherence between the PuM and 10 cortical regions grouped in networks was computed during 5 seconds before and one second after the nociceptive stimulus, and contrasted according to the presence or absence of an arousal EEG response. Pre- and post-stimulus phase coherence between the PuM and all cortical networks was significantly increased in instances of arousal, both during N2 and paradoxical (REM) sleep. Thalamo-cortical enhancement in coherence involved both sensory and higher-level cortical networks and predominated in the pre-stimulus period. The association between pre-stimulus widespread increase in thalamo-cortical coherence and subsequent arousal suggests that the probability of sleep interruption by a noxious stimulus increases when it occurs during phases of enhanced trans-thalamic transfer of information between cortical areas.

Introduction

Being awakened by a noxious stimulus is an objective marker of its intrusiveness. During nocturnal sleep, stimuli disrupting homeostasis can awaken the subject in a very variable proportion of cases, from 30% for nociceptive pricking to 80% in the case of apneas (Bastuji et al., 2008; Lavigne et al., 2000; Lavigne et al., 2004; Chouchou et al., 2014). The probability for a phasic noxious stimulus to disrupt sleep has been found modulated by an increase of pre-stimulus functional connectivity between sensory and higher-level cortical areas (Bastuji et al., 2021) and by the post-stimulus occurrence of a ‘cognitive’ wave (“P3”) reflecting the activation of a widespread cortical network (Bastuji et al., 2008), both in N2 and paradoxical (REM) sleep. Part of such changes in pain responsiveness during sleep might be also linked to functional dissociations between thalamic and cortical activities.

The medial pulvinar (PuM) is an associative nucleus devoid of spinothalamic tract (STT) input, but widely interconnected with regions in parietal, frontal, and temporal lobes,

including higher order and paralimbic association areas (reviews in Cappe et al., 1997; Robinson & Cowie, 1997; Shipp, 2003; Benarroch, 2015). Due to its pattern of widespread and spatially overlapping cortical inputs, PuM is considered as an important node in the trans-thalamic routing of cortico-cortical information (Baleydier & Mauguiere, 1985; Morel et al., 1997; Shipp, 2003; Cappe et al., 2009; Homman-Ludiye & Bourne, 2019)). Its delayed activation after nociceptive stimuli and widespread cortical functional connectivity suggest a role in synchronizing parietal, temporal, and frontal activities, hence contributing to the access of noxious input to conscious awareness (Bastuji et al., 2016a).

Our driving hypothesis in this study was that the functional state of connectivity between the PuM and sensory and high-level cortical areas, could modulate the neural responses to noxious stimuli during sleep, thereby facilitating or inhibiting the subject's awakening. To test this hypothesis, we used intracranial electroencephalographic (iEEG) recordings in epileptic humans to analyse medial pulvinar-cortical functional connectivity (phase-coherence) during the 5 seconds preceding and the second following the delivery of noxious stimuli and correlated them with the occurrence of a potential arousal reaction more than one second after the stimulus.

Subjects and Methods

Patient selection

Eight patients with refractory partial epilepsy were included in the study (5 men, 3 women; mean age 33 years, range 19-51 years). They were consecutive patients agreeing to participate in the study, in accord with their physician in charge and having at least one electrode contact in the PuM. To delineate the extent of the cortical epileptogenic area and to plan a tailored surgical treatment, depth EEG recording electrodes (diameter 0.8 mm; 5-15 recording contacts 2 mm long, inter-contact interval 1.5 mm) were implanted according to the Talairach space (Guénot et al., 2001; Isnard et al., 2018). The procedure aims at recording spontaneous seizures but also includes the functional mapping of potentially eloquent cerebral areas using evoked potentials recordings and cortical electrical stimulation (Ostrowsky et al., 2002; Mazzola et al., 2006). Simultaneous exploration of the thalamus and neo-cortical areas was possible using a single multi-contact electrode, so that thalamic exploration did not increase the risk of the procedure by adding one further electrode track specifically devoted to it. In agreement with French regulations relative to invasive

investigations with direct individual benefit, patients were fully informed about electrode implantation, intracerebral EEG (iEEG) and evoked potential recordings, and cortical stimulation procedures used to localize the epileptogenic cortical areas; and gave their written consent. The laser stimulation paradigm was approved by the local and regional Ethics Committee (CPP Sud Est IV n° 2006-A00572-49).

Spinothalamic-specific laser stimulations were performed during one full night after a minimal delay of five days post electrode implantation; at that time, any 'first-night' effect had faded away, and antiepileptic drugs had been tapered down with daily small doses (see Table 1). None of these patients had chronic pain or reported pain symptoms before or after the recording session.

Electrode implantation

Intracerebral electrodes were implanted using the Talairach's stereotactic frame (Talairach & Bancaud, 1973). A cerebral angiography was performed in stereotactic conditions using an X-ray source located 4.85 m away from the patient's head. This eliminates the linear enlargement due to X-ray divergence and allows a 1:1 scale so that films could be used for measurements without any correction. In a second step, the relevant targets were identified on the patient's MRI, previously enlarged to a scale of one-to-one. As MR and angiographic images were at the same scale, they could easily be superimposed, so as to avoid damage to blood vessels and minimize the risk of haemorrhage during electrode implantation.

Anatomical localization of recording sites

The localization of recording contacts was determined using 2 different procedures. In 4 patients implanted before year 2010, MRI could not be performed with electrodes in place because of the physical characteristics of the stainless-steel contacts. In these cases, the scale 1:1 post implantation skull radiographs performed within the stereotactic frame were superimposed to the pre-implantation scale 1:1 MRI slice corresponding to each electrode track, thus permitting to plot each contact onto the appropriate MRI slice of each patient to determine its coordinates [MRIcro software; (Rorden & Brett, 2000)]. In the other 4 patients, the implanted electrodes were MRI-compatible and cortical contacts could be directly visualized on the post-operative 3D-MRIs. In both cases, anatomical scans were acquired on

a 3-Tesla Siemens Avanto Scanner using a 3D MPRAGE sequence with following parameters: TI/TR/TE 1100/2040/2.95 ms, voxel size: 1 x 1 x 1 mm^3, FOV = 256 x 256 mm^2.

Intracortical electrode contacts were mapped to the standard stereotaxic space (Montreal Neurological Institute, MNI) by processing MRI data with Statistical Parametric Mapping (SPM12 — Wellcome Department of Cognitive Neurology, UK; http:// www.fil.ion.ucl.ac.uk/spm/). Anatomical T1-3D images pre- and post-implantation were co-registered and normalized to the MNI template brain image using a mutual information approach and the segmentation module of SPM12, which segments, corrects bias and spatially normalizes images with respect to the MNI model. Then, the cortical localization of electrodes was performed using a regional atlas (WFU Pickatlas v3) in MRIcro®. In the 4 patients with MRI-compatible electrodes, the cortical contacts could be directly visualized on the post-operative normalized 3D-MRIs. In the 4 patients without MRI-compatible electrodes, the coordinates of contacts were determined on their own pre-operative MRI according to the procedure described above, thus permitting to plot each contact onto the appropriate MRI slice of each patient [MRIcron software] to determine its MNI coordinates. Figure 1 A shows the 52 cerebral contacts from which iEEG signal was recorded and analysed.

Intra-thalamic electrode contacts.

In this work we followed the nomenclature of thalamic nuclei from Hirai and Jones (1989), Morel et al. (1997) and Krauth et al. (2010). The localization of the contacts within the PuM was performed with the appropriate MRI slice of each patient and the Morel's stereotactic atlas of the human thalamus (Morel et al., 1997). In the 4 patients with MRI-compatible electrodes, contacts could be localized according to their positions with respect to the anatomy in each patient, and then projected to the thalamic atlas. In the 4 patients without MRI-compatible electrodes, the coordinates of contacts were determined on their own MRI according to the procedure described above.

Nociceptive-specific laser stimulation.

Radiant nociceptive heat pulses of 5 ms duration were delivered with a Nd:YAP-laser (Yttrium Aluminium Perovskite; wavelength 1.34 µm; El.En.®, Florence, Italy). The laser beam was transmitted from the generator to the stimulating probe via an optical fibre of 10 m length (550µm diameter with sub-miniature version (SAV) A-905 connector). Perceptive and

nociceptive thresholds were determined in each patient immediately before the recording session. Nociceptive thresholds to Aδ stimuli were determined as the minimal laser energy producing a pricking sensation, compared to pulling a hair or receiving a boiling water drop in at least two of three stimuli. They were obtained in all subjects with energy densities between 80 and 100 mJ/mm2, which are within the usual range in our and other's laboratories using Nd:YAP lasers (Cruccu et al., 2008; Kersebaum et al., 2021). These parameters have been validated as being able to activate selectively the spinothalamic system in humans (e.g. Garcia-Larrea et al., 2010; Perchet et al., 2012; La Cesa et al., 2017), including during sleep, where they arouse subjects in ~30% of the cases (Bastuji et al., 2008; Mazza et al., 2012).

Data acquisition and recording procedure.

In each patient, two runs of 10–15 stimulations each were first performed during wakefulness. Interstimulus interval (ISI) was pseudo-randomly adjusted on-line and varied between 10 and 20 s. Stimulus energy was set at the individual nociceptive threshold previously determined and applied to the skin in the superficial radial nerve territory, on the dorsum of the hand contralateral to the hemispheric side of electrodes implantation. The heat spot was slightly shifted over the skin surface between two successive stimuli to avoid both sensitization and peripheral nociceptor fatigue. Two patients were stimulated on the left hand, and 6 on the right hand. Then the patients were allowed to sleep at their own time, and no further laser stimulation was delivered until a minimum of 20 minutes of continuous sleep had been recorded. The identification of the different sleep stages (N2, N3, and PS) was done on-line by one of the investigators (HB) expert in sleep studies. A second investigator entered the room to deliver nociceptive pulses transmitted through the optic fibre from the laser stimulator. If the entrance of the investigator induced EEG changes indicating a sleep shift, an appropriate delay before delivering the stimuli was applied to allow EEG stabilisation. The 10-meter optical fibre transited under the door separating the recording and sleeping areas and allowed to stimulate conveniently the dorsum of the hand despite movements of the subjects during the night. Both the sleeping subject and the investigator wore eye protections. Runs of stimulations were delivered during the different sleep stages up to 6:00 AM. If one stimulus awoke the sleeper the stimulation sequence was immediately discontinued. Recordings were performed during all-night in referential mode,

the reference electrode being chosen for each patient on an implanted contact located in the skull. The iEEG signal was recorded continuously from 96 to 128 channels at a sampling frequency of 256 Hz or 512 Hz, amplified and band pass filtered (0.33-128 Hz; -3dB, 12 dB/octave) to be stored in hard disk for off-line analysis (Micromed SAS®, Macon France).

Sleep scoring and arousal reactions.

Criteria of the American Academy of Sleep Medicine (AASM) adapted to intracerebral recordings (Magnin et al., 2004; Bastuji et al., 2011; Claude et al., 2015) were used for iEEG data. Hypnograms based on 30 s epochs allowed determining the vigilance state during which stimuli were delivered. As already observed in previous studies, laser stimuli delivered during N3 sleep induced quite systematically a shift to N2 sleep stage (Bastuji et al., 2008; 2011); therefore, only recordings from sleep stage N2 and PS are presented here. Following the AASM criteria adapted for intracerebral recordings (Bastuji et al., 2011), "cortical arousals" were defined as bursts of waking cortical activity lasting at least 3 s. These arousal reactions were considered as stimulus-related if they occurred within 10 s after noxious stimulus onset. Signals obtained when stimuli were delivered during an arousal period were rejected.

Inter-areal functional connectivity.

The main steps of iEEG signal processing are illustrated in Figure 1 B-E. Using Brain Analyzer® software, Fast Fourier Transform of the 5 s iEEG signals preceding the stimuli was applied to four spectral bands: delta (1-3), theta (4-7Hz); alpha-sigma (8-15 Hz, mid) and beta-gamma (16-40 Hz, high). Higher gamma frequencies were not included, as they are less involved in long-range coherence relative to lower frequencies (von Stein & Sarnthein, 2000), and are often 'nested' within slower oscillations (Lisman et al., 2013). In each patient, iEEG spectral content was computed for all the brain contacts explored, during both N2 sleep and PS, and stored separately according to the presence (A) or the absence (NA) of an arousal or an awakening reaction after the stimulus. All contacts located within the epileptic network and/or in lesioned tissues were excluded from the analysis.

Pre- and post-stimulus functional connectivity were studied using iEEG phase-coherence analysis, the PuM acting as 'seed region' with respect to cortical areas analysed (MNI coordinates in Table 2). Areas, known to be involved in processing of nociceptive stimuli

(Bastuji et al., 2016b; Bradley et al., 2017; Fauchon et al., 2020) and to be anatomically connected with PuM (review in Homman-Ludiye & Bourne, 2019), were grouped in networks/areas selected for phase-coherence analysis following consensual literature on functional commonalities, and comprised: 1) posterior insula; 2) a 'central executive' network including dorsolateral prefrontal (DLPFC) and posterior parietal (PPC) areas; 3) a 'salience' network including the anterior insula, and mid-cingulate; 4) a 'late-integrative network' including the posterior cingulate-precuneus (PCC, Prec), the perigenual cingulate (pgACC); 5) an 'emotional' network joining orbitofrontal (OFC), amygdala, and hippocampus (Neugebauer et al., 2009; Doucet et al., 2019). Phase-coherence was computed after Fast Fourier Transform, in referential mode, for each spectral band power during the 5 s pre-stimulus signal, and the 100-900 ms after the stimulus. The second time-window was chosen according to previous data obtained with intracerebral recordings showing that evoked responses during sleep are recorded within these latency boundaries (Bastuji et al., 2011; Claude et al., 2015). The phase-coherence value was calculated as the quotient between correlation and autocorrelation for each frequency and each channel pair and underwent Fisher's z'-transformation before statistical analysis, to transform the sampling distribution of coherence values so that it becomes normally distributed (Nunez et al., 1997). Coherence values were computed by calculating the cross-spectrum (a measure of the joint spectral properties of the two channels) normalized by their auto-spectrum (the power spectrum of each channel), as follows:

$$Coh(c_1, c_2)(f) = \frac{|Cov(c_1, c_2)(f)|^2}{|Cov(c_1, c_1)(f)||Cov(c_2, c_2)(f)|}$$

with

$$Cov(c_1, c_2)(f) = \Sigma \left(c_{1,i}(f) - moy\left(c_1(f)\right)\right)\left(c_{2,i}(f) - moy\left(c_2(f)\right)\right)$$

In the second formula, totalling is carried out using the segment number i. The average is obtained with reference to the segment with a fixed frequency f and a fixed channel c.

Statistical analyses.

During N2 sleep individual phase-coherence values between PuM and the different brain networks were submitted to three-way ANOVAs with “arousal” (yes / no), time window (pre-, post-stimulus) and cerebral network (posterior insula, central executive, salience, integrative and emotional), one for each frequency band (delta, theta, mid, high). Similar ANOVAs were performed with phase-coherence values obtained during PS. Post-hoc tests (Holm-Sidak test corrected for multiple comparisons) were applied in case of significant effects following ANOVAs. The reported effect size measure was η^2 in ANOVA and Cohen’s d in t tests.

Statistical analyses were performed with GraphPad Prism 8 and StatView® softwares.

Results

The patients received 67.6 ±38 stimuli during their night sleep and these stimuli were spread over the whole night. The iEEG signals of the 8 patients were obtained from 202 segments during N2 sleep (84 arousal and 118 non-arousal), and from 238 segments during PS (81 arousal and 157 non-arousal). The mean latency of arousals triggered by the stimulus was 1.2 ± 0.05 s in N2 sleep and 0.94 ± 0.07 s in PS. The mean interstimulus interval was 29.2 ± 10.3 s and the interval was not significantly different whether the stimulus gave rise or not to an arousal (28.5 ± 11.7 vs 29.8 ± 9.6; t=0.56; p=0.58).

Spectral phase-coherence during N2 sleep

ANOVA on delta frequency values showed a main effect of arousal on phase-coherence levels between PuM and the five cortical networks, with coherence being significantly enhanced when preceding an arousal reaction (0.48 ± 0.04 vs 0.38 ± 0.04) [F(1,30)=6.44; p=0.017; η^2_p = 0.18] (Figure 2); there was no significant effect of time [F(1,30)=0.27; p=0.61], nor of cerebral network [F(4,30)=0.78; p=0.55]. There was, however, a significant interaction between arousal and time of analysis [F(4,30)=7.37; p=0.0109; η^2_p = 0.20]. This was reflected on post-hoc testing, which showed that coherence in the arousal condition was higher than in ‘no arousal’ during the pre-stimulus phase exclusively, but not during the post-stimulus period (Table 3 & Figure 2).

ANOVA on theta frequency values did not show a main effect of arousal on phase-coherence levels between PuM and the five cortical networks [F(1,30)=2.77; p=0.11], nor of

cerebral network [F(4,30)=1.67; p=0.18]. There was a significant effect of time [F(1,30)=11.24; p=0.0022; η^2_p = 0.27], coherence being higher in pre-stim that in post-stim condition (0.41 ± 0.03 vs 0.31 ± 0.03) (Figure 3). There was also a significant interaction between arousal and time analysis [F(4,30)=17.2; p=0.0003; η^2_p = 0.36]. This was reflected on post-hoc testing, which showed that coherence if an arousal occurred was higher for pre-stimulus condition and not for post-stimulus condition as compared to no arousal (Table 3 & Figure 2).

ANOVA for mid frequency bands (8-15 Hz, alpha-sigma) showed a main effect of arousal on phase-coherence levels between PuM and the five networks, with coherence being significantly enhanced when preceding an arousal reaction (0.40 ± 0.03 vs 0.30 ± 0.02) [F(1,30)=28.36; p<0.0001; η^2_p =0.49] (Figure 2). There was also a significant effect of time [F(1,30)=5.75; p=0.023; η^2_p =0.16], coherence being higher in pre-stim that in post-stim condition (0.39 ± 0.02 vs 0.31 ± 0.03) (Figure 3). There was no effect of cerebral network [F(4,30)=1.91; p=0.14] and no interaction.

ANOVA for high frequency bands (16-40 Hz, beta-gamma) showed a main effect of arousal on phase-coherence between PuM and the five networks, coherence being significantly enhanced when preceding an arousal reaction (0.34 ± 0.03 vs 0.27 ± 0.02) [F(1,30)=10.99; p=0.0024; η^2_p =0.27] (Figure 2). There was no significant effect of time [F(1,30)=3.02; p=0.093], nor of cerebral network [F(4,30)=1.66; p=0.19] and no interaction.

Spectral phase-coherence during PS

ANOVA on delta frequencies did not show a main effect of arousal on phase coherence between PuM and the five networks [F(1,29)=1.48; p=0.23]. Neither was an effect of cerebral network [F(4,29)=0.21; p=0.84], but a significant effect of time [F(1,29)=14.08; p=0.0008; η^2_p = 0.33], coherence being higher in pre-stim that in post-stim condition (0.51 ± 0.04 vs 0.37 ± 0.03) (Figure 3). There was also a significant interaction between arousal and time factors [F(4,29)=8.52; p=0.0067; η^2_p = 0.23], reflected on post-hoc testing by an enhancement of coherence in the arousal condition, exclusively during the pre-stimulus time-window (Table 4; Figure 2).

ANOVA on theta frequencies showed a main effect of arousal on phase coherence between PuM and the five networks [F(1,29)=7.0; p=0.013; η^2_p = 0.19], coherence being

higher in arousal than in non-arousal condition (0.34 ± 0.03 vs 0.25 ± 0.02) (Figure 2). There was also a significant effect of time [F(1,29)=55.3; p<0.0001; η^2_p = 0.66], coherence being higher in pre-stim that in post-stim condition (0.39 ± 0.03 vs 0.20 ± 0.02) (Figure 3). There was no effect of cerebral network [F(4,29)=1.17; p=0.35], and no interaction (Table 4; Figure 2).

ANOVA mid frequency bands (8-15 Hz, alpha-sigma) showed a main effect of arousal on phase-coherence levels between PuM and the five networks (0.38 ± 0.03 vs 0.26 ± 0.02) [F(1,29)=16.03; p=0.0004; η^2_p =0.36] (Figure 2). There was also a significant effect of time analysis [F(1,29)=17.70; p=0.0002; η^2_p =0.38], coherence being higher in pre-stim that in post-stim condition (0.39 ± 0.03 vs 0.26 ± 0.03) (Figure 3), but no effect of cerebral network [F(4,29)=0.81; p=0.53]. There was a significant interaction between arousal and time factors [F(4,29)=11.02; p=0.0024; η^2_p =0.28], reflected on post-hoc testing by an increase of coherence in the arousal condition, which was higher in pre-stimulus than in post-stimulus time-window (Table 4; Figure 2).

ANOVA for high frequency bands (16-40 Hz, beta-gamma) showed a main effect of arousal on phase-coherence levels between PuM and the five networks (0.33 ± 0.02 vs 0.24 ± 0.02) [F(1,29)=22.94; p<0.0001; η^2_p =0.44] (Figure 2). There was also a significant effect of time [F(1,29)=23.68; p<0.0001; η^2_p =0.45], coherence being higher during the pre-stim than the post-stim time window (0.36 ± 0.02 vs 0.25 ± 0.02) (Figure 3), but no effect of cerebral network [F(4,29)=0.69; p=0.60]. There was a significant interaction between arousal and time factors [F(4,29)=9.12; p=0.0052; η^2_p =0.24], reflected on post-hoc testing by an increase of coherence in the arousal condition, which was higher in pre-stimulus than in post-stimulus time-window (Table 4; Figure 2).

In summary, in both N2 sleep and PS a main effect of arousal on coherence values was observed for frequencies covering 8-40 Hz, whereby coherence was significantly enhanced when the stimulus entailed an arousal. For lower frequencies, a main effect of arousal on coherence values was observed for delta in N2 sleep, and for theta in PS. Also, in 7 out of 8 comparisons (2 sleep stages x 4 bands) there was an effect of the time of analysis, coherences being significantly higher preceding the stimulus than following it, either as a main effect or in post-hoc following significant interactions (Figures 2 & 3)

Discussion

The probability for a phasic noxious stimulus to entail an arousal was modulated by the pre- and post-stimulus phase-coherence between medial pulvinar and other cortical areas. Pre-stimulus phase-coherence between the PuM and other cerebral areas was higher in case of arousal to nociceptive stimuli, for all frequency bands and during both N2 and paradoxical sleep. Post-stimulus phase coherence was more complex, higher for alpha-sigma band in N2 sleep and PS, and for beta-gamma band in PS only. The pattern of functional connectivity between PuM and cortical structures, both sensory and of higher order, suggests a role of the associative thalamus in modulating the probability of arousal by nociceptive stimuli.

PuM and its widespread connectivity

The existence of functional relationships between the PuM and a variety of cortical areas is compatible with what is known about the anatomical connectivity of this thalamic nucleus. The PuM is anatomically connected with an extremely wide array of cortical structures including the posterior insula (Mufson & Mesulam, 1984; Burton & Jones, 1976), the posterior and anterior cingulate (Baleydier & Mauguière, 1985; 1987; Romanski et al., 1997), as well as with the amygdala (Jones & Burton, 1976; Romanski et al., 1997), the hippocampus (Baleydier & Mauguière, 1985; Insausti et al., 1987), and a wide collection of frontal and parietal cortical sectors (Trojanowski & Jacobson, 1975; Yeterian & Pandya, 1988; Barbas et al., 1991; Romanski et al., 1997; Gutierrez et al., 2000; Baleydier & Mauguiere, 1977; 1987; Yeterian & Pandya, 1985; Schmahmann & Pandya, 1990 ; Baleydier & Morel, 1992; Hardy & Lynch, 1992; Cappe et al., 2007). During wakefulness, the PuM is activated by nociceptive stimuli (Bastuji et al 2016a), but in accordance with the lack of direct spinothalamic afferents to this nucleus, its responses occur at longer latencies than those of sensory thalamic nuclei, suggesting a dependence on descending cortico-thalamic projections rather than on ascending input (Bastuji et al., 2016a). Indeed, the association of lack of STT afferents, late activation, and widest cortical connectivity is consistent with the associative attributes and anatomical interconnections of PuM with regions in parietal, frontal, and temporal lobes, including higher order cortices and paralimbic association's

areas (reviews in Cappe et al., 1997; Robinson & Cowie, 1997; Shipp, 2003; Benarroch, 2015). This supports a role for the PuM in synchronizing spatially dispersed cortical activities, possibly contributing to the access of noxious input to conscious awareness (Bastuji et al., 2016a).

Due to its pattern of widespread and spatially overlapping cortical inputs, the PuM is considered as an important node in the trans-thalamic routing of cortico-cortical input (Baleydier & Mauguière, 1985; Morel et al., 1997; Shipp, 2003; Cappe et al., 2009). Cortico-thalamic feed-forward projections combined with a subsequent thalamo-cortical transmission is viewed as a fast and secure mode ensuring the transfer of information between remote cortical districts, through a "cortico-thalamo-cortical" route (Guillery, 1995; Rouiller & Welker, 2000; Sherman, 2007; Cappe et al.; 2009). This suggests a role of the PuM nucleus in synchronizing activities of distant cortical areas, hence sustaining the formation of synchronized trans-areal assemblies and contributing to the ultimate access of noxious input to conscious awareness and to favour arousal reaction in case of sleep.

A similar involvement of different cortical networks

Arousal-related changes in functional connectivity with PuM did not differ significantly across the different cortical networks explored, suggesting that the association between arousal and thalamo-cortical coherence is mediated by a widespread modulation of cortical activation, rather than a specific action upon a particular area. This is similar to what was observed in a previous study which investigated arousal-related coherence changes between sensory and associative networks (Bastuji et al., 2021), and suggests that the mechanisms involved in these processes may differ in sleep and wakefulness. Indeed metabolic and electrophysiological studies in the waking state indicate that perceiving stimuli as subjectively painful may depend on the *regional* activation in anterior insula, anterior cingulate and amygdala (Boly et al., 2007; Ploner et al., 2010; Wiech et al., 2010, Gélébart et al., 2022), and/or pre-stimulus EEG phase-coherence between parasylvian and anterior cingulate regions (Ohara et al., 2008). In contrast, during sleep no specific network appears to be precisely associated to the occurrence of arousal reactions. The results of the present study suggest that associative thalamic nuclei, and in particular the PuM, may influence the functional connectivity between sensory and higher-order cortical networks involved in

stimulus processing, including executive, integrative and emotion-related areas, driving them to a favourable state of receptiveness to process input from sensory cortices (Bastuji et al., 2016a, b; Garcia-Larrea & Bastuji, 2018; Bastuji et al., 2021).

Arousal-related coherence changes predominate in the pre-stimulus period

In the pre-stimulus condition, the functional connectivity between the PuM and cortical networks was always significantly higher before an arousal as compared to non-arousal, both for N2 sleep and PS and for each frequency band. This was not the case in the post-stimulus condition, during which phase coherence was enhanced for mid bands in N2 sleep and PS, for delta in N2 sleep only, and for theta and high band in PS only. While we cannot rule out a sampling fluctuation due to the small number of subjects, this may also indicate a real difference in the mechanisms at play immediately before and immediately after the sensory stimulus. Evoked responses following noxious stimuli were found to include a 'cognitive' wave ("P3") in case of arousal, occurring just before the arousal reaction (Bastuji et al., 2008). "P3-like" EEG components reflect the activation of a widespread cortical network including most of the network areas included in the present work (Halgren et al., 1998; Polich, 2007; Huang et al., 2015). P3-like components in depth-recordings have been described in the thalamus (Yingling & Hosobuchi, 1984; Katayama et al., 1985; Velasco et al., 1986; Kropotov & Ponomarev, 1991; Rektor et al., 2001; Klostermann et al., 2006), even if the involvement of the PuM itself was not clearly stated in any of these reports.

Limitations and Perspectives

Our results were obtained in epileptic patients, i.e. subjects with putatively abnormal episodic brain function (spikes, seizures), which may represent a bias. All these patients, however, had nociceptive thresholds in the normal range, and their intracranial responses to noxious stimuli during waking were similar to those obtained on surface recordings with source reconstruction in control subjects (Bradley et al., 2017). These patients were on anti-epileptic drugs, which may alter brain metabolism and induce impairments in brain networks connectivity (Van Veenendaal et al., 2017). Although such limitations are certain and unavoidable, the results reported here are based on *intra- individual* comparisons across

vigilance states, hence we believe that the comparison of phase coherence levels are robust and reliable. Other limitations derive from the fact that functional links determined through phase-coherence analysis do not prove direct causal influences of one structure on another, and we cannot exclude that they may result from functional connections through intermediary regions not recorded here (e.g. Liu et al., 2011). The data we present, although extensive, could not provide a full view of all cortical regions responding to noxious input; in particular, areas of the temporal lobe were not included in analyses due to their frequent involvement in the epileptic process. Their activity may also be relevant for determining arousal, but could not be assessed in this study.

N2 sleep and PS are not homogeneous states but have phasic and tonic components, which might affect differentially stimulus processing. Specific comparisons between sub-stages were not included in analyses to reduce the number of repeated tests and keep statistical power. Our group has previously shown that phasic N2 periods (i.e. those containing spindles) have no differential effects on nociceptive arousal relative to tonic periods (Claude et al., 2015), and that noxious responses in paradoxical sleep do not change between tonic and phasic periods (Bastuji et al., 2008).

Lastly, we did not extend our coherence analysis to high-gamma ranges since phase synchronization of high-gamma activity (>40 Hz) appears restricted to small interareal distances, and declines dramatically for longer ranges, whereas coherence in delta, theta and alpha bands, remains significant (e.g. von Stein & Sarnthein, 2000). Since our coherence analysis focused on widely spaced networks, we opted to concentrate on frequency ranges more likely conveying distant information (Lisman et al., 2013).

Conclusion

Altogether, the results of the present study indicate that the level of functional communication between the associative thalamus (PuM) and a widespread array of cerebral areas immediately prior a noxious stimulus may greatly influence the behavioural responsiveness to the incoming input, by facilitating or hindering the transfer of information necessary to disrupt sleep.

Acknowledgments

Supported by the French Society for Pain Evaluation and Therapy (SFETD Translational Research Grant 2012-14), the LABEX CORTEX (ANR-11-LABX-0042; ANR-11-IDEX-0007), a Region Rhone-Alpes/France ARC2 2012-2015 scholarship and a INSERM Interface Grant to H.B.

Abbreviations list

A: arousal; NA: non arousal

iEEG: intracerebral electroencephalography

MRI: magnetic resonance imagery

P3: P300 component

PuM: medial pulvinar

PS: paradoxical sleep

REM: rapid eye movement

STT: spinothalamic tract

References

Baleydier, C., & Mauguière, F. (1977). Pulvinar-latero posterior afferents to cortical area 7 in monkeys demonstrated by horseradish peroxidase tracing technique. *Experimental Brain Research*, 27:501-7.

Baleydier, C., & Mauguière, F. (1985). Anatomical evidence for medial pulvinar connections with the posterior cingulate cortex, the retrosplenial area, and the posterior parahippocampal gyrus in monkeys. *Journal of Comparative Neurology*, 232:219-28.

Baleydier, C., & Mauguière, F. (1987). Network organization of the connectivity between parietal area 7, posterior cingulate cortex and medial pulvinar nucleus: a double fluorescent tracer study in monkey. *Experimental Brain Research,* 66:385-93.

Baleydier, C., & Morel, A. (1992). Segregated thalamocortical pathways to inferior parietal and inferotemporal cortex in macaque monkey. *Visual Neuroscience*, 8:391-405.

Barbas, H., Henion, T.H., Dermon, C.R. (1991). Diverse thalamic projections to the prefrontal cortex in the rhesus monkey. *Journal of Comparative Neurology,* 313:65-94.

Bastuji, H., Frot, M., Mazza, S., Perchet, C., Magnin, M., Garcia-Larrea, L. (2016a). Thalamic Responses to Nociceptive-Specific Input in Humans: Functional Dichotomies and Thalamo-Cortical Connectivity. *Cerebral Cortex*, 26:2663-76.

Bastuji, H., Frot, M., Perchet, C., Magnin, M., Garcia-Larrea, L. (2016b). Pain networks from the inside: Spatiotemporal analysis of brain responses leading from nociception to conscious perception. *Human Brain Mapping*, 37:4301-4315.

Bastuji, H., Mazza, S., Perchet, C., Frot, M., Mauguière, F., Magnin, M., Garcia-Larrea, L. (2011). Filtering the reality: Functional dissociation of lateral and medial pain systems during sleep in humans. *Human Brain Mapping*, 33:2638–2649.

Bastuji, H., Perchet, C., Legrain, V., Montes, C., Garcia-Larrea, L. (2008). Laser evoked responses to painful stimulation persist during sleep and predict subsequent arousals. *Pain,* 137:589–599.

Bastuji, H., Cadic-Melchior, A., Magnin, M., Garcia-Larrea, L. (2021). Intracortical Functional Connectivity Predicts Arousal to Noxious Stimuli during Sleep in Humans. *The Journal of Neuroscience,* 41:5115-5123.

Benarroch, E.E. (2015). Pulvinar: associative role in cortical function and clinical correlations. *Neurology*, 84:738-47.

Boly, M., Balteau, E., Schnakers, C., Degueldre, C., Moonen, G., Luxen, A., Phillips, C., Peigneux, P., Maquet, P., Laureys, S. (2007). Baseline brain activity fluctuations predict somatosensory perception in humans. *Proceedings of the National Academy of Sciences USA*, 104:12187–12192.

Bradley, C., Bastuji, H., Garcia-Larrea, L. (2017). Evidence-based source modeling of nociceptive cortical responses: A direct comparison of scalp and intracranial activity in humans. *Human Brain Mapping*, 124:168.

Burton, H., & Jones, E.G. (1976). The posterior thalamic region and its cortical projection in New World and Old World monkeys. *Journal of Comparative Neurology,* 168:249-301.

Cappe, C., Morel, A., Rouiller, E.M. (1997). Thalamocortical and the dual pattern of corticothalamic projections of the posterior parietal cortex in macaque monkeys. *Neuroscience*, 146:1371-87.

Cappe, C., Morel, A., Barone, P., Rouiller, E.M. (2009). The thalamocortical projection systems in primate: an anatomical support for multisensory and sensorimotor interplay. *Cerebral Cortex*, 19:2025-37.

Chouchou, F., Pichot, V., Barthélémy, J.C., Bastuji, H., Roche, F. (2014). Cardiac sympathetic modulation in response to apneas/hypopneas through heart rate variability analysis. *PLoS ONE*, 9:e86434.

Claude, L., Chouchou, F., Prados, G., Castro, M., De Blay, B., Perchet, C., Garcia-Larrea, L., Mazza, S., Bastuji, H. (2015). Sleep spindles and human cortical nociception: a surface

and intracerebral electrophysiological study. *Journal of Physiology (Lond)*, 593:4995–5008.

Cruccu, G., Aminoff, M.J., Curio, G., Guerit, J.M., Kakigi, R., Mauguiere, F., Rossini, P.M., Treede, R.D., Garcia-Larrea, L. (2008). Recommendations for the clinical use of somatosensory-evoked potentials. *Clinical Neurophysiology*, 119:1705–1719.

Doucet, G.E., Lee, W.H., Frangou, S. (2019). Evaluation of the spatial variability in the major resting-state networks across human brain functional atlases. *Human Brain Mapping,* 40:4577–4587.

Fauchon, C., Meunier, D., Faillenot, I., Pomares, F.B., Bastuji, H., Garcia-Larrea, L., Peyron, R. (2020). The Modular Organization of Pain Brain Networks: An fMRI Graph Analysis Informed by Intracranial EEG. *Cerebral Cortex Communication*, 1:tgaa088.

Garcia-Larrea, L., & Bastuji, H. (2018). Pain and consciousness. Progress in *Neuropsychopharmacology and Biological Psychiatry*, 87:193-199.

Garcia-Larrea, L., Perchet, C., Creac'h, C., Convers, P., Peyron, R., Laurent, B., Mauguiere, F., Magnin, M. (2010). Operculo-insular pain (parasylvian pain): a distinct central pain syndrome. *Brain*, 133:2528–2539.

Gélébart, J., Garcia-Larrea, L., Frot, M. (2022). Amygdala and anterior insula control the passage from nociception to pain. Cerebral Cortex, bhac290.

Guénot, M., Isnard, J., Ryvlin, P., Fischer, C., Ostrowsky, K., Mauguiere, F., Sindou, M. (2001). Neurophysiological monitoring for epilepsy surgery: the Talairach SEEG method. StereoElectroEncephaloGraphy. Indications, results, complications and therapeutic applications in a series of 100 consecutive cases. *Stereotactic and Functional Neurosurgery,* 77:29–32.

Guillery, R.W. (1995). Anatomical evidence concerning the role of the thalamus in corticocortical communication: a brief review. *Journal of Anatomy*, 187:583-92.

Gutierrez, C., Cola, M.G., Seltzer, B., Cusick, C. (2000.) Neurochemical and connectional organization of the dorsal pulvinar complex in monkeys. *Journal of Comparative Neurology,* 419:61-86.

Halgren, E., Marinkovic, K., Chauvel, P. (1998). Generators of the late cognitive potentials in auditory and visual oddball tasks. *Electroencephalography and Clinical Neurophysiology*, 106:156-64.

Hardy, S.G., & Lynch, J.C. (1992). The spatial distribution of pulvinar neurons that project to two subregions of the inferior parietal lobule in the macaque. *Cerebral Cortex*, 2:217-30.

Hirai, T., & Jones, E.G. (1989). A new parcellation of the human thalamus on the basis of histochemical staining. *Brain Research Review*, 14:1-34.

Homman-Ludiye, J., Bourne, J.A. (2019). The medial pulvinar: function, origin and association with neurodevelopmental disorders. *Journal of Anatomy*, 235:507-520.

Huang, W.J., Chen, W.W., Zhang, X. (2015). The neurophysiology of P 300--an integrated review. *European Review for Medical and Pharmacological Sciences*, 19:1480-8.

Insausti, R., Amaral, D.G., Cowan, W.M. (1987). The entorhinal cortex of the monkey: III. Subcortical afferents. *Journal of Comparative Neurology,* 264:396-408.

Isnard, J. et al. (2018). French guidelines on stereoelectroencephalography (SEEG). *Neurophysiologie Clinique/Clinical Neurophysiology*, 48:5–13.

Jones, E.G., & Burton, H. (1976). A projection from the medial pulvinar to the amygdala in primates. *Brain Research*, 104:142-7.

Katayama, Y., Tsukiyama, T., Tsubokawa, T. (1985). Thalamic negativity associated with the endogenous late positive component of cerebral evoked potentials (P300): recordings using discriminative aversive conditioning in humans and cats. *Brain Research Bulletin*, 14:223-6.

Kersebaum, D., Fabig, S.C., Sendel, M., Muntean, A.C., Baron, R., Hüllemann, P. (2021). Revealing the time course of laser-evoked potential habituation by high temporal resolution analysis. *European Journal of Pain,* 25:2112-2128.

Klostermann, F., Wahl, M., Marzinzik, F., Schneider, G.H., Kupsch, A., Curio, G. (2006). Mental chronometry of target detection: human thalamus leads cortex. *Brain*, 129: 923-31.

Krauth, A., Blanc, R., Poveda, A., Jeanmonod, D., Morel, A., Székely, G. (2010). A mean three-dimensional atlas of the human thalamus: Generation from multiple histological data. *Neuroimage*, 49: 2053-2062.

Kropotov, J.D., & Ponomarev, V.A. (1991). Subcortical neuronal correlates of component P300 in man. *Electroencephalography and Clinical Neurophysiology,* 78:40-9.

La Cesa, S., Di Stefano, G., Leone, C., Pepe, A., Galosi, E., Alu, F., Fasolino, A., Cruccu, G., Valeriani, M., Truini, A. (2017). Skin denervation does not alter cortical potentials to surface concentric electrode stimulation: A comparison with laser evoked potentials and contact heat evoked potentials. *European Journal of Pain*, 22:161–169.

Lavigne, G. (2004). Experimental pain perception remains equally active over all sleep stages. *Pain*, 110:646–655.

Lavigne, G., Zucconi, M., Castronovo, C., Manzini, C., Marchettini, P., Smirne, S. (2000). Sleep arousal response to experimental thermal stimulation during sleep in human subjects free of pain and sleep problems. *Pain*, 84:283–290.

Lisman, J.E., & Jensen, O. (2013). The teta-gamma neural code. *Neuron*, 77:1002-16.

Liu, C.C., Shi, C.Q., Franaszczuk, P.J., Crone, N.E., Schretlen, D., Ohara, S., Lenz, F.A. (2011). Painful laser stimuli induce directed functional interactions within and between the human amygdala and hippocampus. *Neuroscience*, 178:208–217.

Magnin, M., Bastuji, H., Garcia-Larrea, L., Mauguière, F. (2004). Human thalamic medial pulvinar nucleus is not activated during paradoxical sleep. *Cerebral Cortex*, 14:858–862.

Mazza, S., Magnin, M., Bastuji, H. (2012). Pain and sleep: from reaction to action. *Neurophysiologie Clinique/Clinical Neurophysiology,* 42:337-44.

Mazzola, L., Isnard, J., Mauguiere, F. (2006). Somatosensory and pain responses to stimulation of the second somatosensory area (SII) in humans. A comparison with SI and insular responses. *Cerebral Cortex*, 16:960–968.

Morel, A., Magnin, M., Jeanmonod, D. (1997). Multiarchitectonic and stereotactic atlas of the human thalamus. *The Journal of Comparative Neurology*, 387:588-630.

Mufson, E.J., & Mesulam, M.M. (1984). Thalamic connections of the insula in the rhesus monkey and comments on the paralimbic connectivity of the medial pulvinar nucleus. *The Journal of Comparative Neurology*, 227:109-20.

Neugebauer, V., Galhardo, V., Maione, S., Mackey, S.C. (2009). Forebrain pain mechanisms. *Brain Research Reviews*, 60:226–242.

Nunez, P.L., Srinivasan, R., Westdorp, A.F., Wijesinghe, R.S., Tucker, D.M., Silberstein, R.B., Cadusch, P.J. (1997). EEG coherency. I: Statistics, reference electrode, volume conduction, Laplacians, cortical imaging, and interpretation at multiple scales. *Electroencephalography and Clinical Neurophysiology,* 103:499–515.

Ohara, S., Crone, N.E., Weiss, N., Kim, J.H., Lenz, F.A. (2008). Analysis of synchrony demonstrates that the presence of “pain networks” prior to a noxious stimulus can enable the perception of pain in response to that stimulus. *Experimental Brain Research*, 185:353–358.

Ostrowsky, K., Magnin, M., Ryvlin, P., Isnard, J., Guénot, M., Mauguière, F. (2002). Representation of pain and somatic sensation in the human insula: a study of responses to direct electrical cortical stimulation. *Cerebral Cortex*, 12:376–385.

Perchet, C., Frot, M., Charmarty, A., Flores, C., Mazza, S., Magnin, M., Garcia-Larrea, L. (2012). Do we activate specifically somatosensory thin fibres with the concentric planar electrode? A scalp and intracranial EEG study. *Pain*, 153:1–9.

Ploner, M., Lee, M.C., Wiech, K., Bingel, U., Tracey, I. (2010). Prestimulus functional connectivity determines pain perception in humans. *Proceedings of the National Academy of Sciences USA*, 107:355–360.

Polich, J. (2007). Updating P300: an integrative theory of P3a and P3b. *Clinical Neurophysiology*, 118:2128-48.

Rektor, I., Kanovsky, P., Bares, M., Louvel, J., Lamarche, M. (2001). Event-related potentials, CNV, readiness potential, and movement accompanying potential recorded from posterior thalamus in human subjects. A SEEG study. *Neurophysiologie Clinique/Clinical Neurophysiology,* 31:253-61.

Robinson, D.L., & Cowie, R.J. (1997). The primate pulvinar: structural, functional, and behavioral components of visual salience. In Steriade M, Jones EG, McCormick DA, editors. Thalamus Vol II Experimental and Clinical Aspects (Elsevier, Oxford). pp 53-92.

Romanski, L.M., Giguere, M., Bates, J.F., Goldman-Rakic, P.S. (1997). Topographic organization of medial pulvinar connections with the prefrontal cortex in the rhesus monkey. *The Journal of Comparative Neurology,* 379:313-32.

Rorden, C., & Brett, M. (2000). Stereotaxic display of brain lesions. *Behavioural Neurology*, 12:191–200.

Rouiller, E.M., Welker, E. (2000). A comparative analysis of the morphology of corticothalamic projections in mammals. *Brain Research Bulletin*, 53:727-41.

Schmahmann, J.D., & Pandya, D.N. (1990). Anatomical investigation of projections from thalamus to posterior parietal cortex in the rhesus monkey: a WGA-HRP and fluorescent tracer study. *The Journal of Comparative Neurology,* 295:299-326.

Sherman, S.M. (2007). The thalamus is more than just a relay. *Current Opinion in Neurobiology,* 17:417-22.

Shipp, S. (2003). The functional logic of cortico-pulvinar connections. *Philosophical Transactions of the Royal Society of London. Series B: Biological Sciences*, 358:1605-24.

von Stein, A., & Sarnthein, J. (2000). Different frequencies for different scales of cortical integration: from local gamma to long range alpha/theta synchronization. *International Journal of Psychophysiology*, 38:301-13.

Talairach, J., & Bancaud, J. (1973). Stereotaxic approach to epilepsy. Methodology of anatomo-functional stereotaxic investigations. *Progress in Neurological Surgery*, 5: 297–354.

Trojanowski, J.Q., Jacobson, S. (1975). A combined horseradish peroxidase-autoradiographic investigation of reciprocal connections between superior temporal gyrus and pulvinar in squirrel monkey. *Brain Research*, 85:347-53.

van Veenendaal, T.M., IJff, D.M., Aldenkamp, A.P., Lazeron, R.H.C., Hofman, P.A.M., de Louw, A.J.A., Backes, W.H., Jansen, J.F.A. (2017). Chronic antiepileptic drug use and functional network efficiency: A functional magnetic resonance imaging study. *World Journal of Radiology,* 28:287-294.

Velasco, M., Velasco, F., Velasco, A.L., Almanza, X., Olvera, A. (1986). Subcortical correlates of the P300 potential complex in man to auditory stimuli. *Electroencephalography and Clinical Neurophysiology,* 64:199-210.

Wiech, K., Lin, C.S., Brodersen, K.H., Bingel, U., Ploner, M., Tracey, I. (2010). Anterior insula integrates information about salience into perceptual decisions about pain. *Journal of Neuroscience,* 30:16324–16331.

Yeterian, E.H., & Pandya, D.N. (1985). Corticothalamic connections of the posterior parietal cortex in the rhesus monkey. *The Journal of Comparative Neurology,* 237:408-26.

Yeterian, E.H., & Pandya, D.N. (1988). Corticothalamic connections of paralimbic regions in the rhesus monkey. *The Journal of Comparative Neurology,* 269:130-46.

Yingling, C.D., & Hosobuchi, Y. (1984). A subcortical correlate of P300 in man. *Electroencephalography and Clinical Neurophysiology,* 59:72-6.

Table 1. Individual clinical, MRI and iEEG data

Patient	**Gender/Age**	**Treatment** (mg/day before-after tapering)	**MRI**	**Seizure onset**	**Number of Electrodes R: right; L: left**
P1	M/19	Carbamazepine 1200-800 Valproate 1000-500 Clobazam 10-10	R fronto-orbital	R fronto-orbital	11/R
P2	F/23	Levetiracetam 2000-1000 Lamotrigine 800-300	L hippocampal atrophy	L mesial temporal	11/L
P3	F/37	Carbamazepine 1600-600 Pregabalin 300-75	Normal	L mesial temporal	13/L
P4	F/51	Oxcarbazepine 600-200 Clobazam 20-10	Normal	R temporal	12/R
P5	M/26	Carbamazepine 1000-200 Lamotrigine 400-200 Pregabalin 300-75	L hippocampal atrophy	L mesial temporal	12/L
P6	M/39	Lamotrigine 400-200 Topiramate 300-200 Levetiracetam 3000-1000 Lacosamide 200-100	L hippocampal atrophy	L mesial temporal	11/L
P7	M/32	Levetiracetam 1500-1000 Oxcarbazepine 750-150	L hippocampal atrophy	L basal temporal	13/L+2/R
P8	M/37	Carbamazepine 800-400 Topiramate 400-200 Clobazam 10-5	Normal	L perisylvian	13/L

Table 2 : MNI coordinates (x, y, z) of cerebral contacts.

Contacts	P insula (n=8)	Thal (n=8)	DLPFC (n=4)	PPC (n=4)	A insula (n=4)	MCC (n=3)	PCC (n=6)	Precun (n=3)	Hippo (n=3)	OFC (n=3)	Amygd (n=6)
Patients											
P1	37,-20,5	16,-28,8		52,-48,46		4,29,22	5,-48,18	5,-48,46			21,-3,-18
P2	37,-24,2	17,-29,8		45,-55,41			3,-48,23	8,-55,41			20,-6,-23
P3	35,-23,5	18,-23,5	50,22,23	37,-53,45	33,6,12	4,22,28	4,-50,20			5,46,-14	
P4	37,-1,-4	11,-25,8			38,16,1		10,-45,25		22,-15,-25		15,-6,-20
P5	33,-23,5	17, -24, 4	30,44,11		32,2,8	6,4,36					
P6	36,-25,1	22,-26,1		39,-60,45			9,-52,26	14,-63,45	29,-31,-6		21,-9,-26
P7	36,-12,-1	11,-26,4	40,36,0				6,-42,31		29,-18,-16	4,54,1	17,0,-11
P8	37,-12,2	11,-27,5	42,48,9		35,8,5					7,48,-11	24,-2,-21
Mean	**36,-18,2**	**15,-26,5**	**40,38,11**	**43,-54,44**	**35,8,7**	**5,18,29**	**6,-48,24**	**9,-55,44**	**27,-21,-16**	**5,49,-8**	**20,-4,-20**
SD	**1,8,3**	**4,2,3**	**8,11,9**	**8,5,2**	**3,6,5**	**1,13,7**	**3,4,5**	**5,8,3**	**4,9,10**	**2,4,8**	**3,3,5**

Table 3. N2 sleep: post hoc analyses of phase-coherence values with respect to the significant interaction between arousal and time. t, p and d values if significant

Time window	Delta No-Arousal/Arousal	Theta No-Arousal/Arousal
Pre-stimulus	t(34)=3.61; p<0.002; d=0.71	t(34)=3.86; p=0.001; d=0.74
Post-stimulus	t(34)=0.18; p=0.86	t(34)=1.47; p=0.15

Table 4. Paradoxical Sleep: post hoc analyses of phase-coherence values with respect to the significant interaction between arousal and time. t, p and d values if significant

Time window	Delta No-Arousal/Arousal	Theta	Alpha-sigma No-Arousal/Arousal	Beta-gamma No-Arousal/Arousal
Pre-stimulus	t(33)=2.54; p=0.032; d=0.48	t(33)=2.76; p=0.019; d=0.76	t(33)=5.31; p<0.0001; d=0.94	t(33)=5.65; p<0.0001; d=1.22
Post-stimulus	t(33)=0.46; p=0.65	t(33)=0.1.79; p=0.08	t(33)=2.08; p=0.046; d=0.27	t(33)=3.28; p=0.0025; d=0.40

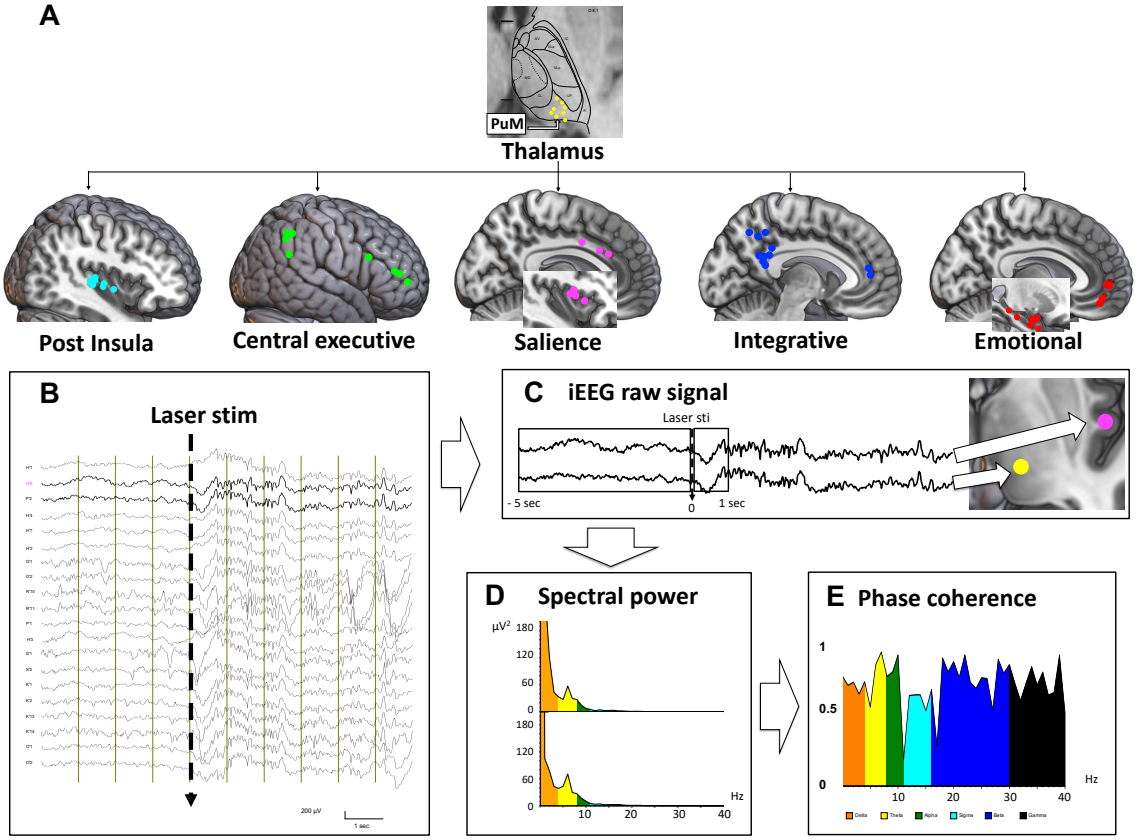

Figure 1. A. Localization of recording contacts used for analysis in each area represented on MNI Brain templates, and on Morel thalamic atlas for the medial pulvinar (PuM): **Top:** PuM. **Bottom: from left to right**: posterior insula (n=8); central executive network with posterior parietal cortex (n=4) and dorsolateral prefrontal cortex (n=4); salience network with anterior insula (n=4) and mid cingulate (n=3); integrative network with posterior cingulate (n=6), precuneus (n=3) and perigenual cingulate (n=2); emotional network with hippocampus (n=3), amygdala (n=6)and orbitofrontal (n=4). **B**. Example of iEEG traces before and after a laser stimulus. **C.** Two iEEG signals obtained before and after the laser stimulus, one in the PuM and the other in the posterior insula. Rectangles indicate the analysis periods, of 5 sec before and 1 sec after the stimulus respectively. On the MRI slice black and cyan circles represent the localization of these two contacts. **D.** Spectral powers of both iEEG signals during the periods analysed. **E.** Phase-coherence between signal recorded simultaneously in the PuM and the posterior insula.

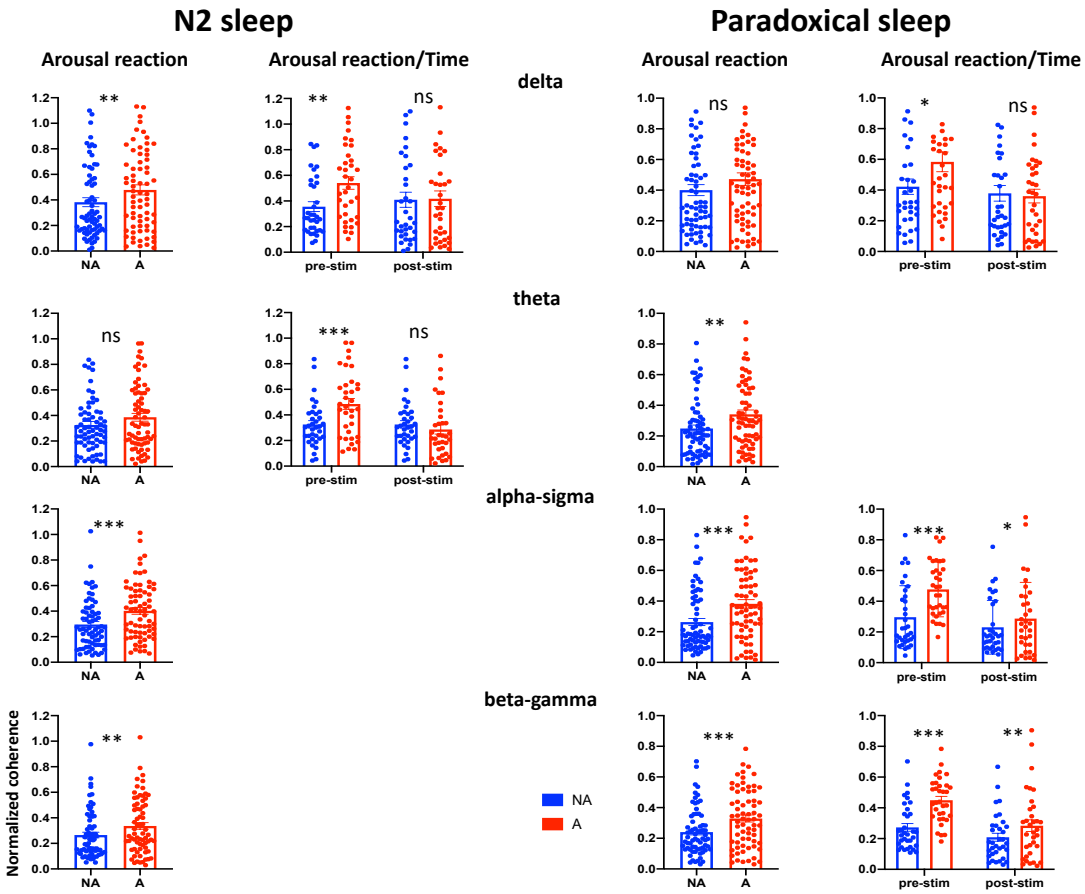

Figure 2. Pre- and post-stimulus spectral phase coherence according to the presence or absence of an arousal reaction. Phase-coherence levels (scatter plot, mean± SEM) of the 4 frequency bands in the two sleep stages (Left: N2 sleep; Right: PS) according to the presence (red) or absence (blue) of an arousal. For both N2 and PS sections, the left column depicts results from the two analysis periods pooled together, while the right column the results are separated into pre- and post-stimulus periods. Note that the ordinates scales are different for N2 sleep and PS.

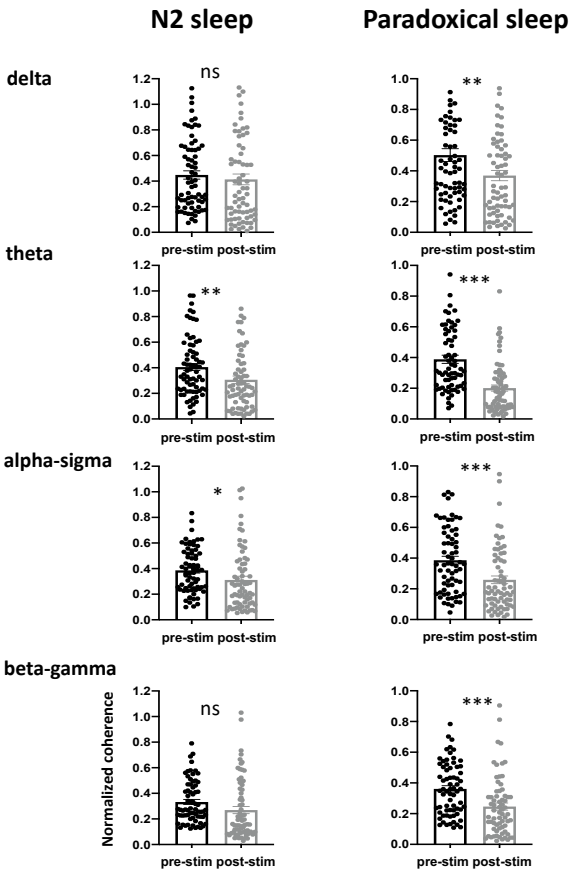

Figure 3. Spectral phase coherence between PuM and each of the cerebral networks according to time periods.

Phase-coherence levels (scatter plot, mean ± SEM) of iEEG for delta, theta, alpha-sigma and beta-gamma between PuM and the 5 networks/areas during N2 sleep (left) and PS (right) according to time periods. Phase-coherence values during the pre- (black) and post-stimulus (grey) periods. Note that the ordinates scales are different for N2 sleep and PS.